

Modeling and Control of Micro-grid Powered by Solar and Wind Energies

Sameh Zenned¹, Emna Aridhi², Abdelkader Mami³

^{1,2,3} Department of Physics, Faculty of Sciences of Tunis, Farhat Hached University, Tunisia

Article Info

Article history:

Received Oct 29, 2016

Revised Jan 04, 2016

Accepted Jan 14, 2017

Keyword:

Battery

Micro-Grid

MPPT

Photovoltaic

Wind turbine

ABSTRACT

The number of installations of Micro-Grid or intelligent micro power networks will increase to quadruple by 2020. The purpose is to reduce the cost and the consumption of electricity in transmission and distribution networks, using a hybrid system powered by solar and wind sources, as well as integrating storage devices. This paper reviews and discusses the Micro-Grid Model. It describes various Micro-Grid components and different configurations. It also presents the model of two generation units (Photovoltaic and Wind Turbine). Then, a comparative study of different battery types used for large-scale electricity storage is carried out, followed by a review of control strategies.

Copyright © 2017 Institute of Advanced Engineering and Science.
All rights reserved.

Corresponding Author:

Zenned Sameh,

Department of Physics, Faculté des Sciences de Tunis Université de Tunis El Manar,

Campus Universitaire Farhat Hached,

El Manar, Tunis 2092, Tunisie.

Email: zennedsameh@yahoo.fr

Nomenclature

I_{ph} Photovoltaic current (A)

P_{pv} Power output of PV array (P)

I_{pvc} Output current of the PV cell (A)

I_s Saturation current

I_{cc} Short-circuit current (A)

I_r Solar irradiance (W/m^2)

V_{pvc} Output voltage of the PV cell (V)

I_{wind} DC current leaving the PWM inverter

V_{wind} Wind speed (m/s)

P_{wind} Wind power (w)

T_{wind} Aerodynamic torque (Nm)

(V_a, V_b, V_c) Three-phase stator voltage

(I_a, I_b, I_c) Three-phase stator currents

V_d, V_q Instantaneous stator voltages in dq0-axes

I_d, I_q Instantaneous stator currents in dq0-axes

V_{DC} DC bus voltage

1. INTRODUCTION

Micro-grid (MG) is defined as a voltage distribution network with distributed renewable energy sources (RES), storage devices and loads. Generally, MG could be operated in either grid-connected or stand-alone [1]-[3]. In the literature, several combination of RES have been proposed, such as, Wind Turbine (WT)/DG (Diesel Generator) [4], Photovoltaic (PV)/FC (Fuel Cell), WT/PV [1],[5]-[9], WT/PV/DG [8],[10], WT/PV/FC/MT (Micro-Turbine) [3], PV/DG [11], PV/WT/FC [1].

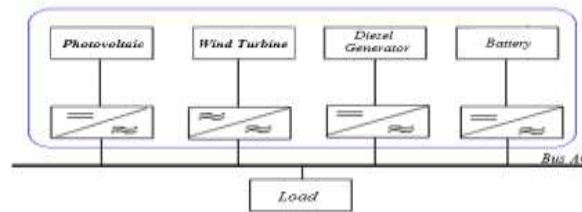


Figure 1. Example of a Microgrid injected into the AC bus

Most of MG installations are based on power electronic components to provide the required flexibility, to ensure a controlled operation as a single aggregated system, and to meet the local needs of customers. The electrical power system supports the continuous operation of various components and power systems. At present, there is a need to build an extensive library of MG components in the standard simulation environment. Hence, it involves the development of adequate models for simulation of distributed generators and short-term storage, as well as the configuration of power electronic interfaces.

According to the Renewables Global Status Report (GSR) released in 2015 [12], the most rapid growth, and the largest increase in capacity occurred in the power sector, led by wind, solar PV, and hydropower. In 2014, solar PV marked another growth year record, with an estimated 40 GW installed for a total global capacity of about 177 GW [13]. The global wind power market added a record of 51 GW in order to obtain a global power capacity of 370 GW [13]. Photovoltaic and wind are the most invested in the recent technologies. In terms of dollars committed, the solar and wind power account for more than 55% and 36.8% of new investment in renewable power and fuels, respectively. Both sustained significant increase over 2013: the solar and wind power investment increased of 25% (149.5 billion), and 11% (99.5 billion), respectively. Consequently, more than a quarter of new investment in renewable energy went to small-scale projects (particularly solar PV) during 2014 [13].

Table 1. Important indicators for renewable energy

Power	unit	2012	2013	2014
Solar PV capacity	GW	100	139	177
Wind power capacity	GW	283	319	370
Hydropower capacity	GW	960	1015	1055

The micro sources are constituted by a photovoltaic generator, a wind turbine, a DC voltage source, and a battery used as an energy storage unit. They are also equipped with a Maximum Power Point Tracker (MPPT) able to meet the real and reactive power control within pre-specified limits. Thus, the present paper focused on presenting the models used for simulation of Microgrid components. It is organized as follows: Section 2 presents models used in the library for different components, such as PV arrays, and wind turbines that integrate the Microgrid. Section 3, the different types of batteries used for a large scale energy storage are discussed. Finally, section 4 focuses on a review of Microgrid control techniques, taking into account the voltage and current inverter models.

2. MODELING OF RENEWABLE ENERGY SOURCES FOR MICROGRID

Hybrid PV and WG system becomes a very attractive solution, especially for stand-alone applications. According to several techno-economic studies, the combination of the PV and WG sources allows a better performance of the HRP system.

2.1. Photovoltaic Generation

PV modules are semiconductor components that use photo-electric properties to generate electrical power. The behavior of PV cells can be modeled with an equivalent circuit shown in Figure 2.

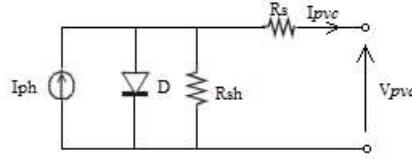


Figure 2. Equivalent Circuit of PV Cell

The panel consists of photovoltaic cells characterized by a photovoltaic current I_{ph} , a diode, a serial resistance R_s and a shunt resistance R_{sh} . Hence, the cell output current I_{pvc} is expressed by:

$$I_{pvc} = I_{ph} - I_s \left[\exp \left(\frac{V_{pvc} - R_s I_{pvc}}{V_t} \right) - 1 \right] - \frac{V_{pvc} - R_s I_{pvc}}{R_{sh}} \tag{1}$$

V_t is the temperature dependent thermal voltage, and given by:

$$V_t = \frac{AKT}{q} \tag{2}$$

with, V_t is the thermodynamic potential where is temperature dependent variable, A is the ideality factor, K is the Boltzmann constant ($1.3806 \cdot 10^{-23} J/K$), T is the operating temperature, and q is the electron charge ($1.6022 \cdot 10^{-19} C$). The photovoltaic current is defined in (3).

$$I_{ph} = \frac{I_r}{1000} \left[I_{ph0} + \frac{\partial I_{pv}}{\partial T_c} (T_c - 25) \right] \tag{3}$$

where, I_{ph0} is a constant by the short-circuit value I_{cc} of the panels, $\frac{\partial I_{pv}}{\partial T_c}$ is provided in the manufacturer data, and T_c is the internal temperature of the cell, which is computed using (4).

$$T_c = T_{atm} + \frac{I_r}{800} (NOCT - 20) \tag{4}$$

with, T_{atm} is the atmospheric temperature, I_r is the solar irradiance, NOCT is a manufacturer data designating the internal operating temperature of the cell for $T_{atm} = 20^\circ C$, and $I_r = 800 W/m^2$. The equation between the generator current I_{pv} and the output voltage V_{pv} is defined in (5).

$$I_{pv} = N_p \left[I_{ph} - I_s \left[\exp \left(\frac{1}{V_t} \left(\frac{V_{pv} + R_s I_{pv}}{N_s + \frac{R_s I_{pv}}{N_p}} \right) \right) - 1 \right] \right] - \frac{N_p V_{pv}}{N_s R_{sh}} - \frac{R_s I_{pv}}{R_{sh}} \tag{5}$$

To provide the maximum power, a permanent adaptation of the load with the photovoltaic generator is necessary. This adaptation can be achieved by the insertion of a DC-DC converter (chopper) controlled by a tracking mechanism "Maximum Power Point Tracking" (MPPT) presented in Figure 4.

The power output of a PV array is based on the solar irradiance and the ambient temperature. The power output in this model is calculated using (6).

$$P_{pv} = \eta_{pvg} A_{pvg} I_r \tag{6}$$

where, η_{pvg} is the PV generation efficiency, A_{pvg} is the PV generator area (m^2), and I_r is the solar irradiation entitled module plane (W/m^2). η_{pvg} is further defined as:

$$\eta_{pv\&g} = \eta_r \eta_{pc} \left[1 - \beta (T_c - T_{ref}) \right] \quad (7)$$

where, η_{pc} is the power conditioning efficiency. It is equal to one when the MPPT is used, β is temperature coefficient ((0.004-0.006) per °C), η_r is the reference module efficiency, and T_{ref} is the reference cell temperature (°C).

Many DC-DC converters are designed to connect a photovoltaic panel, which injects the PV energy into the electrical grid. It is presented in Figure 3. Several of research works used DC-DC converters to elevate the voltage to the DC bus voltage level of the system. For instance, Hasan et al [14] proposed a Cùk converter in order to extract at the solar power out of the PV arrays with high stability [15]. For the purpose of assessing the duty cycles of Cùk, an MPPT controller is used. This converter is the most suitable DC chopper for evaluating a ripple free current in the PV side. The energy transfer from the source to the load is continuous regardless of the MOSFET switchstate. By comparing with SEPIC (Single Ended Primary Inductor Converter) based on an MPPT system, the dynamic performance with Cùk converter is also satisfactory [16]. In addition, the results also show that the Cùk converter based on the MPPT controller is more efficient than the existing MPPT controller system recently proposed [17]. Baptista et al [18] presented a new DC-DC converter in order to connect a photovoltaic panel. Nowadays, modern society applies for fully integrated solutions in order to decrease costs and improve the energy efficiency. Furthermore, the increasingly worldwide use of residential appliances imposes researchers to find technology solutions to guarantee a near 100% reliable power grid system.

DC-DC converters, as power management devices, must comply with these recent technological and industrial trends. A hybrid Boost/Cùk converter is proposed. It makes possible to get high voltage gains with just one controlled power semiconductor. The basic design equations of the Boost/Cùk converter are determined by supposing that the used components are ideal. Secondly, losses are introduced and quantified to obtain the converter efficiency leading to the converter design for a specified efficiency. In this case, a Boost/Cùk converter was studied. An efficiency of 96.01% and an output voltage of 450.3 V (0.07% of error) are reached. In order to maintain the converter operation properly, two control systems are developed. The operation is ensured by a MPPT algorithm, and then by a DC voltage control system. Both approaches are implemented and tested. Indeed, they were mixed in an integrated system that was successfully tested. The output voltage and the PV power delivered to the converter are maintained to 450V and 650W, respectively. Sheng-Yu Tseng et al [19] developed a power system using a high step-up converter for DC load applications. The high step-up converter adopts a boost converter [20].

Two interleaved active clamp boost converters with coupled inductor are adopted to form a PV power system for DC load applications. They are powered by PV arrays and batteries and have been proposed to implement MPPT and power management. Furthermore, a microchip associated with PWM IC is used to implement maximum power point tracking operation, voltage regulation and power management. Choudhary et al [21] proposed a standalone PV system connected with buck converter and Incremental Conductance algorithm to extract the maximum power at different environmental conditions. They used the high frequency DC-DC Buck converter in order to interface the PV panel with the load. The DC-DC buck converter converts a higher DC input voltage to a lower DC output voltage. It consists of a controlled switch, an uncontrolled switch diode, an inductor, a capacitance, and a load resistance. The complete model is divided into three parts: the PV model, the IC MPPT method and the DC-DC Buck converter. The duty ratio for the converter is determined by the MPPT algorithm based on the solar irradiation and a prevailing ambient condition. The DC-DC buck converter is designed to operate at 25 kHz. Hence, the results obtained at different environmental conditions show a good agreement with the experimental ones. The steady state was reached fastly using the MPPT algorithm.

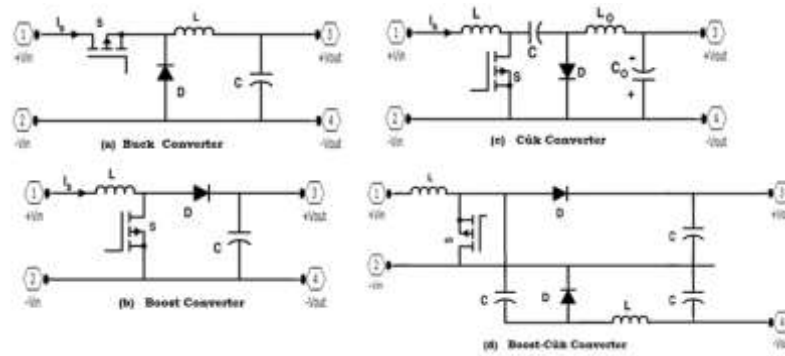


Figure 3. DC-DC Converters: (a) Buck Converter, (b) Boost Converter, (c) Cuk Converter, (d) Boost-Cuk Converter

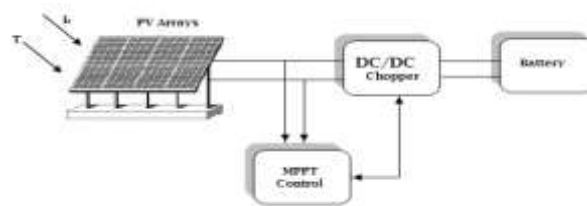


Figure 4. Photovoltaic Model

2.2. Wind Power Generation

Wind turbines are used to convert the wind power into an electrical power that is plotted in Figure 6. It can be classified according to physical features such as dimensions, axes, number of blades, generated power, as well as their orientation and their axis of rotation, into horizontal and vertical axis wind turbines, which can be installed on the land or sea [22]. The wind energy conversion is divided into fixed and variable speeds. In case where the speed is fixed, the generator is directly coupled to the network. Its speed is imposed by the grid frequency and the number of pairs of the generator poles. We have distinguished two wind turbines with technology fixed speed: wind turbines with aerodynamic stall and wind turbines with directional propellers. Sometimes, the mechanical speed is slightly high than to the synchronism speed. Hence, it is necessary to add a multiplier to adjust the generator of the wind turbine rotor. Consequently, the mechanical variable speed should depend on the wind speed to extract the maximum power generated. Two structures of wind turbines with a variable speed are developed: The first is based on the asynchronous machine cage, allowing the stator to operate at variable speed by static converters. the second is based on a double-fed asynchronous machine and wound rotor. The variable speed is achieved using power converters, located on the rotor circuit.

On the other hand, the wind turbine is characterized by a polynomial function C_p , which is determined using different methods, such as blade element method [23], look-up table [24] and analytical approximation [25], λ is defined in (8).

$$\lambda = \frac{R\omega_m}{V_{wind}} \tag{8}$$

Where, V_{wind} is the wind speed (m/s), R is the blades radius (m), ω_m is the angular speed (m/s). The wind power captured by the turbine is expressed in (9).

$$P_{wind} = T_{wind}\omega_m = \frac{1}{2} \rho_{air} C_p(\lambda) S V_{wind}^3 \tag{9}$$

Where, ρ_{air} is the air density and S is the area of wind turbine. It is computed using (10).

$$S = 2RH \quad (10)$$

with, H is the height of blades (m). In the literature, the probability distribution of wind speed is developed by the Weibull distribution and was accepted without any statistical survey [26]. it presents a better adjustment of the wind speed data. The Weibull distribution is characterized by two parameters, one is the shape parameter k and the other is the scale parameter c (m/s). The cumulative distribution function and the probability function are given by (11) and (12), respectively.

$$F(v) = 1 - \exp\left[-\left(\frac{v}{c}\right)^k\right] \quad (11)$$

$$f(v) = \frac{dF(v)}{dv} = \frac{k}{c} \left(\frac{v}{c}\right)^{k-1} \exp\left[-\left(\frac{v}{c}\right)^k\right] \quad (12)$$

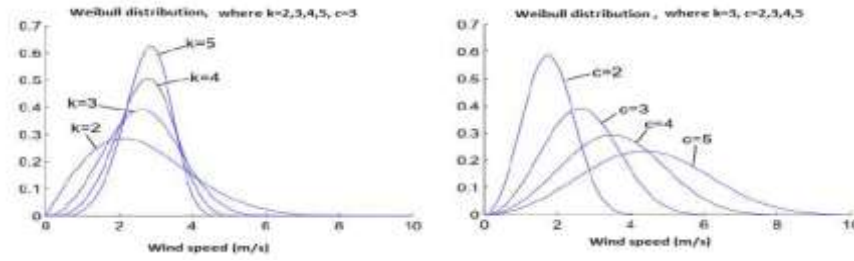


Figure 5. Weibull distribution, (a) according to k , (b) according to c

The angular velocity is presented in (13).

$$J \dot{\omega}_m + f \omega_m = T_{wind} - T_{em} \quad (13)$$

where, J is the inertia of the wind power system, f is the frictional resistance, T_{em} is the electromagnetic torque, created by the wind generator and calculated using (14).

$$T_{em} = \frac{3}{2} p \phi I_q \quad (14)$$

where, p is the number of pairs of poles, and ϕ is the magnetic flux magnitude of each permanent magnet (Wb/m^2). The DC current I_{wind} leaving the PWM inverter is computed according to the power using (15).

$$I_{wind} = \frac{I_a V_a + I_b V_b + I_c V_c}{V_{DC}} = \frac{I_d V_d + I_q V_q}{V_{DC}} \quad (15)$$

where, (V_a, V_b, V_c) are the instantaneous a , b , and c three-phase stator voltages and (I_a, I_b, I_c) are the instantaneous three-phase stator currents. $(V_d$ and $V_q)$ are the instantaneous stator voltages in the dq -axes reference frame, and $(I_d$ and $I_q)$ are the instantaneous stator currents in the dq -axes reference frame.

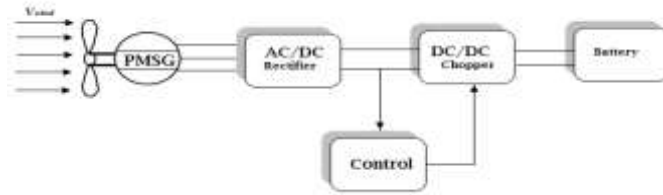


Figure 6. Wind Turbine Model

3. A REVIEW OF LARGE-SCALE BATTERY STORAGE

In this section, a technical comparison between the different types of large-scale batteries is presented [27]. Table 2 gives the technical characteristics of each energy storage system. In addition, their advantages and disadvantages are listed in Table 3.

Table 2. Technical characteristics of large scale energy storage systems

Technology	Power rating (MW)	Discharge duration	Response time	Efficiency (%)	Lifetime
Lead–acid batteries	<50	1min-8h	<1/4 cycle	85	3-12 years
Nickel–cadmium batteries	<50	1min-8h	N/A	60-70	15-20 years
Sodium–sulfur batteries	<350	<8h	N/A	75-86	5 years
Zinc–bromine flow batteries	<1	<4h	1/4 cycle	75	2000 cycles
Flywheels	<1.65	3-120s	<1 cycle	90	20 years
Pumped hydro energy storage systems	100-400	4-12h	s-min	70-85	30-50 years
Compressed air energy storage systems	100-300	6-20h	s-min	64	30 years

The lithium-ion batteries and sodium–sulfur batteries have high power and energy density, as well as a high efficiency. However, they have high production costs. Moreover, pumped hydro energy storage systems and compressed air energy storage systems have a high capacity. Nonetheless, they have special site requirements.

The energy applications of sodium–sulfur batteries, pumped hydro energy storage systems and compressed air energy storage systems are able to provide the energy very quickly in the power system. Nonetheless, the other energy storage systems like Lead-acid batteries, etc are not practical and economic [28].

Table 3. Comparison of large scale energy storage systems

Battery Type	Advantages	Disadvantages
Lead–acid batteries	Low power density and capital cost	Limited life cycle when deeply Discharged
Lithium-ion batteries	High power and energy densities, high efficiency	High production cost, requires special charging circuit
Sodium–sulfur batteries	High power and energy densities, high efficiency	Production cost, safety concerns (addressed in design)
Flywheels	High efficiency and power density	Low energy density
Pumped hydro energy storage systems	High capacity	Special site requirement
Compressed air energy storage systems	High capacity, low cost	Special site requirement, needs gas fuel

Battery energy storage systems are mainly used as ancillary services or to support the large-scale wind and solar integration into the existing electrical system, as well as to ensure the network stability, the frequency regulation and the wind smoothing solar energy [29]. Table 4 illustrates the worldwide battery applications mostly used.

Table 4. Applications of the Battery Storage in the Word

Energy storage	Project	Loacation	System / Size Mwe / Mwh
Lead–acid batteries	- Berliner Kraft Und Licht Battery Storage	Germany	8.5 - 14
Nickel–cadmium batteries	- AES West cover Coal fired power Station	NewYork (USA)	20- N/A
	- KWP II Kaheawa Wind Power II Project	Hawai, USA	10- 20
Sodium–sulfur batteries	- Amplex Group	U.A.E.	350-N/A
	- TEPCO Tokyo Electric Power Company	Japan	200- N/A
Lithium-ion batteries	- Zhangbei	China	20 - 36
	- Laurel Mountain	West Virginia, USA	

The analysis has shown that the large battery energy storage systems use Sodium-sulfur batteries [28]. These systems are mainly used to support integration in a hybrid solar and wind system by providing grid stability, frequency regulation, voltage support, power quality, load shifting, and energy arbitrage. The comparison between the different types of batteries, and the other types of large scale energy storage systems, showed that Lithium-ion and Sodium-sulfur batteries have high power and energy densities, as well as a good efficiency.

The Sodium-sulfur (NAS) battery is an advanced secondary battery that is developed by Tokyo Electric Power Company (TEPCO) and NGK Insulators. The equivalent electrical circuit of the battery is presented in Figure 7.

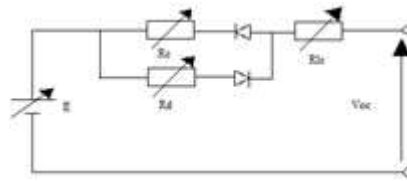


Figure 7. NaS Battery

4. A REVIEW OF MICROGRID CONTROL TECHNIQUES

The productionsystems must ensure energy autonomy by the maximization of the power recovered by the sources. Thus, we propose a review of the control strategies for a hybrid power system constituted by a photovoltaic generator, a wind generator and a battery storage.

4.1. A Review of MPPT Techniques for Photovoltaic Generator

First, the maximum power point of a photovoltaic generator should be tracked. The MPPT depends on irradiance and the temperature. The voltage-current relationship and the power voltage are a nonlinear relationship, as shown in Figure 8.

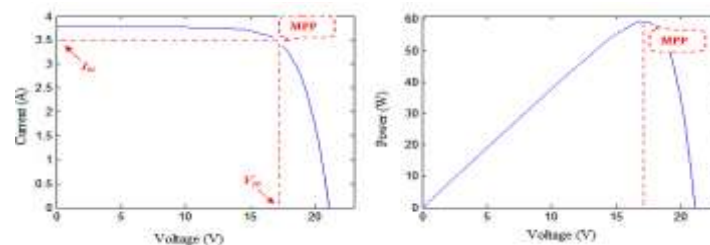


Figure 8. Characteristics of PV cell: (a) voltage-current characteristic, (b) voltage-power characteristic

There are several techniques to extract the maximum power point tracking, such as:

4.1.1. Perturb and Observe

Perturb and Observe is the most commonly used MPPT method seen that is easy to implement and has a high efficiency [17],[30]. The objective is to maximize the power, to increase the maximum voltage

without lowering the current. The algorithm is running until the maximum power point is reached. It consists of searching the power optimum value [31], and is depicted in Figure 9.

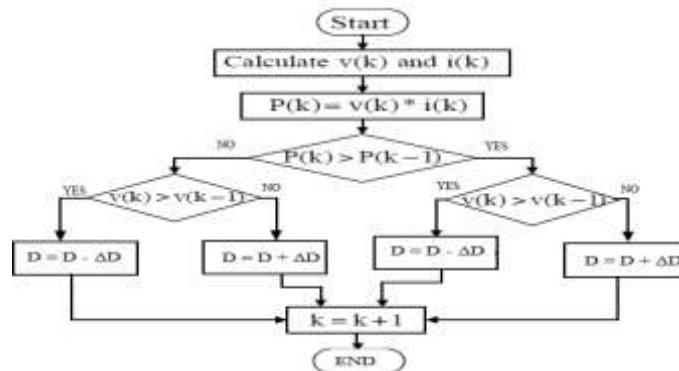


Figure 9. P&O Algorithm

4.1.2. Incremental Conductance Method

The Incremental Conductance Method is an alternative to the Perturb and Observe method where, the Photovoltaic terminal voltage is adjusted according to the MPP voltage by determining $(\frac{dI}{dV}$ and $\frac{I}{V})$, [30]-[31], using (16) and (17).

$$\frac{dP}{dV} = \frac{d(VI)}{dV} = I + V \frac{dI}{dV} = 0 \tag{16}$$

$$-\frac{I}{V} = \frac{dI}{dV} \tag{17}$$

where, $-\frac{I}{V}$ of equation (17) represents the opposite of the PV array instantaneous conductance, and $\frac{dI}{dV}$ represents its incremental conductance. The advantage of this algorithm, compared with the P&O method, is the fast power tracking process. However, the disadvantage is the instability, that can be happened due to the use of a derivative operation in the algorithm depicted in Figure 10.

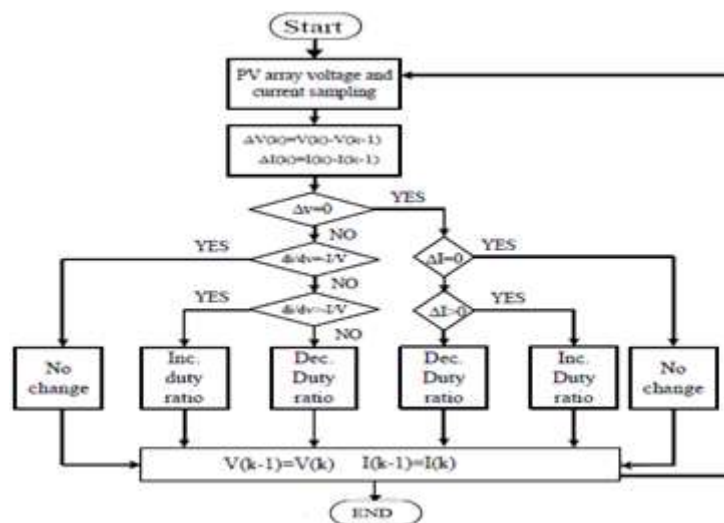


Figure 10. Incremental Conductance Algorithm

4.1.3. Parasitic Capacitance Algorithm

Similar to incremental conductance method, the parasitic capacitance algorithm is developed by Salas et al [31], which highlight the parasitic junction capacitances of the PV panel. It is modeled as a capacitor that is parallel connected to each PV cell in a module. By adding this capacitance to the lighted diode equation (5), (18) is obtained.

$$I_{pv} = F(v_{pv}) + C_p \frac{dv_{pv}}{dt} \quad (18)$$

where, $F(v_{pv})$ is a function of voltage, $C_p \frac{dv_{pv}}{dt}$ presented the current in the parasitic capacitance. This method is faster than the P&O. However, it presents bad results at low irradiation.

4.1.4. Open and Short Circuit Approach

This method of the MPP determination is based on the real time measure of the current in short-circuits or of the open-circuit voltage, using predefined Current-Tension curves [32]. This method presents two advantages: the rapid response to the fluctuations and the absence of variations in steady state. However, this method cannot produce the maximum power available from the PV arrays.

4.1.5. Fuzzy logic control

The fuzzy logic control is increasingly used [8],[33]. Its advantage that does not need any mathematical model of the system, is able to handle the system non-linearity, gives a robust performance under parameter variation, load and supply voltage disturbances. Hence, the cost is reduced. In addition, the input to fuzzy controller is an error signal, E, and the change in error CE. It has three stages: Fuzzification (determining the degree of memberships in each fuzzy partition), Inference (using of rules triggered by the different inputs), and Defuzzification (the passage of fuzzy values of outputs to a net final value). Finally, two variables are measured: output voltage and current of the DC/DC converter.

4.1.6. Neural network

The neural network approach is presented by Zhang [34] and Yaichi [35]. To guarantee an accurate MPPT operation, the neural network operates with the PV generator and adjusts for time varying characteristics of the system. It does not require detail information about the PV system, like a black box model.

4.2. A Review of MPPT Techniques for Wind Generator

This section reviews states of the MPPT algorithms for wind energy systems [36]. Due to the wind changing, the determination of a generator optimal value is difficult. Therefore, there are various control strategies to track the maximum power of the wind turbine systems. The algorithms can be classified as either with or without sensors, as well as according to the techniques used to locate the maximum peak. Shirmohammadi et al [37] proposed a comparison of MPPT algorithms for wind energy systems. Some examples of MPPT algorithms are reported.

4.2.1. Tip Speed Ratio method

The first algorithm Tip Speed Ratio (TSR) is presented in Figure 11. The TSR method changes the generator speed to maintain the reference tip speed ratio. The reference TSR can be determined experimentally or theoretically, and stored as a reference. This method is very simple. However, it requires the wind speed measurement and the wind turbine characteristics [38].

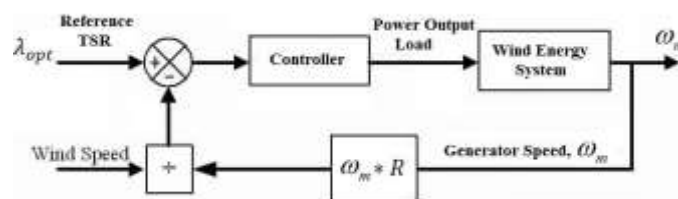


Figure 111. Block Diagram of the TSR Control

The optimum power is written in (19).

$$P_{\max} = K_{opt} * \omega_{opt}^3 \tag{19}$$

where, $K_{opt} = \frac{1}{2} \rho_{air} S \left(\frac{R}{\lambda_{opt}} \right)^3 C_{p,\max}$, and $\omega_{opt} = \frac{\lambda_{opt}}{R} \cdot V$

4.2.2. Optimal Torque control

The method of Optimal Torque (OT) control is described in Figure 12. This method adjusts the PMSG torque according to a maximum power reference torque of the wind turbine at a given wind speed. For any wind speed, the MPPT device imposes a torque reference able to extract the maximum power [39].

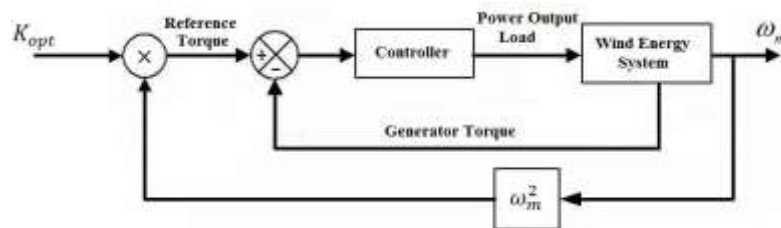


Figure 12. Block Diagram of the OT control

The analytical expression of the optimum torque curve is written in (20).

$$T_{opt} = K_{opt} * \omega_{opt}^2 \tag{20}$$

The method of OT is fast and simple. However, its efficiency is lower compared with the TSR control because it does not measure the wind speed directly, which means that the wind changes are not reflected instantaneously [40].

4.2.3. Power Signal Feedback control

Figure 13 shows the block diagram of a wind energy system with Power Signal Feedback (PSF) controller for maximum power extraction. In this control method, the reference optimum power versus shaft speed is stored in a look up table. Thus, the reference optimum power curve of the wind turbine should be obtained first from the experimental results. While implementing the PSF control, the power loss should be considered in order to determine the accurate given maximum power.

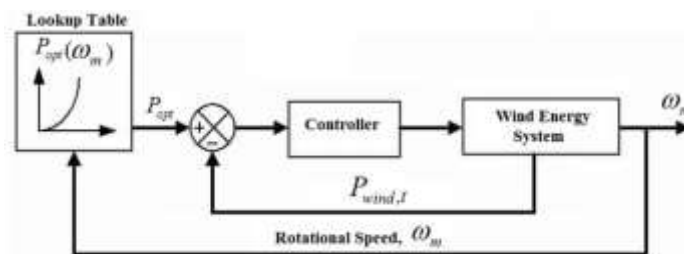


Figure 123. Block Diagram of the PSF Control

The optimal power P_{opt} is determined using (21).

$$P_{opt} = K_{opt} * \omega_m^3 \quad (21)$$

In terms of implementation, Raza and other researchers [40],[41] show that the PSF and OT control methods have the same performance and complexity.

4.2.4. P&O or Hill Climb Searching

The perturbation and observation (P&O), or hill-climb searching (HCS) method, is the most used to determine the optimal operation of wind energy systems. The principle of this method is to perturb a control variable and observe the resulting changes, until the slope becomes zero. It is presented in Figure 14. In the literature, the control variable varies from one author to another: someone used it as a variable rotation speed, and the other used the inverter input voltage.

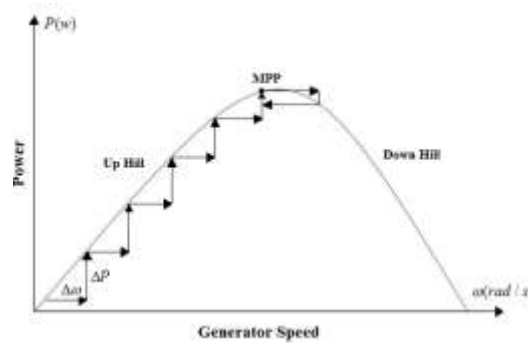


Figure 134. P&O HCS Control

Ying Zhu et al [42] show that the HCS method is an infinite loop even if the MPP value is reached. Then, the speed oscillates around the MPP as shown in Figure 15. Two rules (22) and (23) are proposed to solve this problem.

$$|P(k) - P(k-1)| < \delta \quad (22)$$

$$\left| \frac{P(k) - P(k-1)}{\omega(k) - \omega(k-1)} \right| < \theta \quad (23)$$

The first rule (22) means that the power variation $\Delta P(k)$ should be less than a threshold δ . The second rule (23) means that the gradient of the ω versus P curve should be less than a threshold θ . The climbing search will be stopped when both of the two checks are true and then the MPP is detected [43]. Two problems associated with the conventional HCS, are presented by Shirmohammadi in [37]: the speed efficiency tradeoff and the wrong directionality under rapid wind change.

4.2.5. Fuzzy Logic control

The fuzzy logic is a new theory used to control the wind turbine [8],[33],[37],[44]. It is one of the most effective applications. The fuzzy control method is characterized by a fast convergence, a parameter insensitivity, and an acceptance of noisy and inaccurate signals. It can also be used to obtain an optimal step-size for the conventional HCS method [37]. For instance, Adzic et al [45] describe the FLC applied to an induction generator speed for WT applications. The FLC requires a controller, which will track the wind speed in order to achieve the tip speed ratio λ_{opt} and extract the maximum power. Therefore, the principle of the fuzzy controller is to increment or decrement the generator speed according to the corresponding increment or decrement of the estimated output power. The FLC operation does not need any wind velocity information, and its search is insensitive to the variation of the system parameters.

Salma et al [45] developed a pitch angle control of a wind turbine using a FLC for low rated wind speed, which the block diagram is shown in Figure 15. With the aim of maximizing the power output, the fuzzy controller has been performed with a HCS algorithm. The control of the wind turbine aerodynamic torque is ensured by controlling the pitch. Consequently, it allows improving the performance of the WT mechanical power response compared with the case when the fixed pitch angle is used or without control.

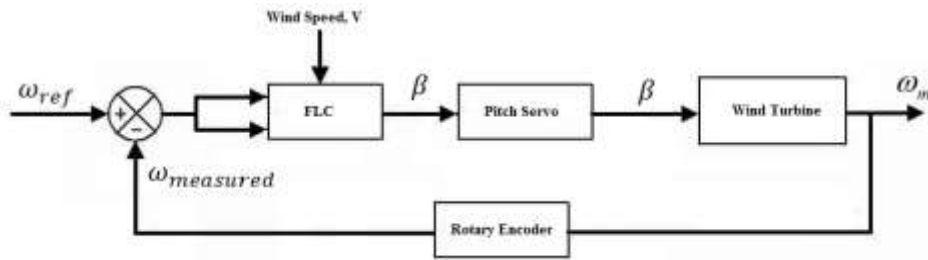


Figure 145. Pitch angle control

5. CONCLUSION

The design of specific micro-network operations requires the study of various technical and economic aspects of network protection. Hence, we must ensure the stability of the microgrid when it is connected or disconnected to the main network. In addition, it requires the protection of the micro-network against the various failures or disruptions happened in the main network. Therefore, it is important to improve the micro-network, such as controlling of the voltage and the power flow, as well as sharing or load shedding and reducing of the electricity network losses. For that purpose, a review study on the modeling of the hybrid power system that is constituted by a photovoltaic array, a wind turbine and batteries, was carried out. The MPPT control methods were also discussed. The study reports that this kind of power systems is the most used and has fewer costs. Moreover, the fuzzy logic control is considered the most efficient compared with the classical control methods, such as the P&O algorithm.

REFERENCES

- [1] J. Salazar, *et al.*, "A Microgrid Library in a General Simulation Language," *The International Federation of Automatic Control Cape Town (IFACCT 2014)*, South Africa, August 24-29, 2014.
- [2] P. Sandeep and M. G. Naik, "Modeling and operation of microgrid with wind and photovoltaic resources," *International Research Journal of Engineering and Technology (IRJET)*, vol/issue: 02(04), 2015.
- [3] G. Chukka, *et al.*, "Modeling and Simulation of Microgrid Connected Renewable Energy Resources with MPPT Controller and by Using SVPWM Technique," *International Research Journal of Engineering and Technology (IRJET)*, vol/issue: 3(1), 2014.
- [4] A. Kanthwal and A. Ganesh, "Hybrid Wind-Diesel Generation System," *International Journal of Applied Engineering Research*, vol/issue: 7(11), 2012.
- [5] R. A. Badwawi, *et al.*, "A Review of Hybrid Solar PV and Wind Energy System," *Smart Science*, vol/issue: 3(3), pp. 127-138, 2015.
- [6] S. Aissou, *et al.*, "Modeling and control of hybrid photovoltaic wind power system with battery storage," *Energy Conversion and Management*, vol. 89, pp. 615-625, 2015.
- [7] S. Kanrav and P. Yadav, "Hybrid power system using wind energy and solar energy," *International Journal of Innovative Research in Science, Engineering and Technology (IJIRSET)*, vol/issue: 5(1), 2016.
- [8] P. Patel and J. Shrivastava, "Modelling & performance analysis of hybrid renewable energy resources using fuzzy logic controller," *International Journal of Science, Engineering and Technology Research*, vol/issue: 5(5), 2016.
- [9] A. Gheiratmand, *et al.*, "Technical and economic evaluation of hybrid wind/PV/battery systems for Off-Grid areas using HOMER Software," *International Journal of Power Electronics and Drive System IJPEDS*, vol/issue: 7(1), pp. 134-143, 2016.
- [10] M. Boussetta, *et al.*, "Dimensionnement optimal d'un système Pv- Eolien-Diesel autonome pour alimenter une ferme agricole dans la région de Sefrou-Maroc," *2ème édition du Congrès International de Génie Industriel et Management des systèmes (CIGIMS'15)*, 2015.
- [11] M. Adouane, *et al.*, "Feasibility study of a hybrid plants (photovoltaic- LPG generator) system for rural electrification," *Renewable Energy and Environmental Sustainability (REES)*, vol/issue: 1(15), 2016.
- [12] Renewable 2015 Global Status Report-REN21, ISBN 978-3-9815934-6-4, REN21, UNEP 15, Rue de Milan F-75441 Paris CEDEX 09 France, www.ren21.net, 2015.
- [13] Renewable 2014 Global Status Report-REN21, ISBN 978-3-9815934-2-6, REN21, UNEP 15, Rue de Milan F-75441 Paris CEDEX 09 France, www.ren21.net, 2014.
- [14] R. Hasan, *et al.*, "Maximum Power Point Tracking Using DC/DC Cuk Converter for Photovoltaic Systems," *International Conference on Materials, Electronics & Information Engineering, ICMEIE-2015*, Faculty of Engineering, University of Rajshahi, Bangladesh, 2015.
- [15] J. Dunia, *et al.*, "Cuk Converter Based Maximum Power Point Tracking for Photovoltaic System Using Incremental Conductance," *International Journal of Innovative Research in Advanced Engineering (IJIRAE)*, vol/issue: 1(11), 2014.

- [16] C. S. Kirthi and S. Karthik, "A Sepic Converter with Linear Transformer and Ripple Free Output for Wide Range Input Applications," *International Journal of Advanced Research in Computer and Communication Engineering*, vol/issue: 4(5), 2015.
- [17] T. P. Sahu, *et al.*, "Simulation and Analysis of Perturb and Observe MPPT Algorithm for PV Array Using Cuk Converter," *Advance in Electronic and Electric Engineering*, vol/issue: 4(2), pp. 213-224, 2014.
- [18] F. Baptista, *et al.*, "Boost/Cuk Converter Using a Single Controlled Power Semiconductor For Photovoltaic Applications," <https://fenix.tecnico.ulisboa.pt>.
- [19] S. Y. Tseng and H. Y. Wang, "A Photovoltaic Power System Using a High Step-up Converter for DC Load Applications," *Energies*, pp. 1068-1100, 2013.
- [20] A. Attou, *et al.*, "Photovoltaic Power Control Using MPPT and Boost Converter," *Balkan Journal of Electrical & Computer Engineering*, vol/issue: 2(1), 2014.
- [21] D. Choudhary and A. R. Saxena, "DC-DC Buck-Converter for MPPT of PV System," *International Journal of Emerging Technology and Advanced Engineering*, vol/issue: 4(7), 2014.
- [22] S. M. Bolik, "Modelling and Analysis of Variable Speed Wind Turbines with Induction Generator during Grid Fault," Alborg University, Denmark, 2004.
- [23] G. Ingram, "Wind Turbine Blade Analysis using the Blade Element Momentum Method," Commons Attribution-ShareAlike 3.0 Unported License, <http://creativecommons.org/licenses/by-sa/3.0/>, October 18, 2011.
- [24] A. W. Manyonge, *et al.*, "Mathematical Modelling of Wind Turbine in a Wind Energy Conversion System: Power Coefficient Analysis," *Applied Mathematical Sciences*, vol/issue: 6(91), pp. 4527-4536, 2012.
- [25] D. Călin and C. Adriana, "Analytical Approximations in modeling of power wind turbines," *Natural Resources and sustainable development*, 2013.
- [26] Y. Ditikovich and A. Kuperman, "Comparison of Three Methods for Wind Turbine Capacity Factor Estimation," *Hindawi Publishing Corporation the Scientific World Journal*, 2014.
- [27] T. Bayar, "Batteries for energy storage: new developments promise grid flexibility and stability," *Renewable Energy World magazine*, 2011.
- [28] A. Poullikkas, "A comparative overview of large-scale battery systems for electricity storage," *Renewable and Sustainable Energy Reviews*, vol. 27, pp. 778-788, 2013.
- [29] REA, "Energy storage in the UK, an overview," www.r-e-a.net, published winter 2015/16, November 2015.
- [30] B. Bhandari, *et al.*, "Mathematical Modeling of Hybrid Renewable Energy System: A Review on Small Hydro-Solar-Wind Power Generation," *International Journal of Engineering and Manufacturing-Green Technology*, vol/issue: 1(2), pp. 157-173, 2014.
- [31] V. Salas, *et al.*, "Review of the maximum power point tracking algorithms for stand-alone photovoltaic systems," *Solar Energy Materials & Solar Cells*, vol. 90, pp. 1555-1578, 2006.
- [32] B. W. Liu and R. Cheung, "Advanced Algorithm for MPPT Control of Photovoltaic System," *Canadian Solar Building Conference*, Montreal, August 2004.
- [33] S. K. A. Shezan, *et al.*, "Fuzzy Logic implementation with MATLAB for solar-wind-battery-diesel hybrid energy system," *Imperial Journal of Interdisciplinary Research (IJIR)*, vol/issue: 2(5), 2016.
- [34] L. Zhang, *et al.*, "Neural Network Based Maximum Power Point Tracking for Grid-Connected Photovoltaic Systems," *International Conference on Power Electronics, Machines and Drives*, vol/issue: 4(7), pp. 18-23, 2002.
- [35] M. Yaichi, *et al.*, "A Neural Network Based MPPT Technique Controller for Photovoltaic Pumping System," *International Journal of Power Electronics and Drive System (IJPEDS)*, vol/issue: 4(2), pp. 241-255, 2014.
- [36] J. S. Thongam and M. Ouhrouche, "MPPT Control Methods in Wind Energy Conversion Systems," *Fundamental and Advanced Topics in Wind Power, FATWP*, 2016.
- [37] R. Shirmohammadi, *et al.*, "The compression of MPPT methods in small sized wind power plants," *Journal of Artificial Intelligence in Electrical Engineering*, vol/issue: 3(11), 2014.
- [38] C. Balasundar, *et al.*, "Design of an Optimal Tip Speed Ratio Control MPPT Algorithm for Standalone WECS," *International Journal for Research in Applied Science & Engineering Technology*, vol/issue: 3(V), 2015.
- [39] A. M. Eltamaly, *et al.*, "Maximum Power Extraction from Utility-Interfaced Wind Turbines," book 'New Developments in Renewable Energy', 2013.
- [40] S. M. R. Kazmi, *et al.*, "Review and critical analysis of the research papers published till date on maximum power point tracking in wind energy conversion system," *IEEE Energy Conversion Congress and Exposition (ECCE)*, pp. 4075-82, 2010.
- [41] M. A. Abdullah, *et al.*, "A review of maximum power point tracking algorithms for wind energy systems," *Renewable and Sustainable Energy Reviews*, vol. 16, pp. 3220-3227, 2012.
- [42] Y. Zhu, *et al.*, "A Novel Maximum Power Point Tracking Control for Permanent Magnet Direct Drive Wind Energy Conversion Systems," *Energies*, vol/issue: 5(5), pp. 1398-1412, 2012.
- [43] T. Salma and R. Yokeeswaran, "Pitch Control of DFIG based Wind Energy Conversion System for Maximum Power Point Tracking," *International Journal of Advanced Research in Electrical, Electronics and Instrumentation Energy*, 2013.
- [44] M. A. Bouzid, *et al.*, "Adaptive Fuzzy Logic Control of Wind Turbine Emulator," *International Journal of Power Electronics and Drive System IJPEDS*, vol/issue: 4(2), pp. 233-240, 2014.
- [45] E. Adzic, *et al.*, "Maximum Power Search in Wind Turbine Based on Fuzzy Logic Control," *Acta Polytechnica Hungarica*, vol/issue: 6(1), 2009.

BIOGRAPHIES OF AUTHORS

Zenned Sameh received the Master's degree in Automatic from the Higher School of Sciences and Techniques of Tunis (ESSTT) in 2010. Currently, she is pursuing the Ph.D. degree in Electronics with the Faculty of Sciences of Tunis, in the Laboratory of Analysis, Design and Control Systems (LACS) at the National School of Engineering of Tunis (ENIT). Her research interests include electrical power systems integrating energy storage devices.



Aridhi Emna received the Ph.D. degree in Electronics from the Faculty of Sciences of Tunis (FST) in 2015. She works on the modelling using bond graph approach of cooling systems and the control of industrial processes, in the Laboratory of Analysis, Design and Control Systems (LACS) at the National School of Engineering of Tunis (ENIT).



Abdelkader Mami received his Dissertation H.D.R (Enabling To Direct Research) from the University of Lille, France, in 2003. He is currently a Professor at the Faculty of Sciences of Tunis (FST) and a Scientific Advisor in the Faculty of Science of Tunis (Tunisia). He is a President of the commutated thesis of electronics in the Faculty of sciences of Tunis, and the person responsible for the research group of analysis and command systems in the ACS laboratory, ENIT, Tunis.